










## Precision and trajectory of three-dimensionally printed animal-specific drill guide for cervical transpedicular screw placement in dogs: An *ex vivo* study

Page 1 a 9

[Precisão e trajetória de guia de perfuração animal-específico impresso tridimensionalmente para colocação de parafusos transpediculares cervicais em cães: um estudo *ex vivo*]

L.F. Sargi<sup>1</sup> , T.A.S.S. Rocha<sup>2</sup> , A. Dissenha<sup>1</sup> , F.B. Silva Sobrinho<sup>1</sup> ,  
J.A. Gonçalves Neto<sup>1</sup> , L.G.G.G. Dias<sup>1</sup> , B.W. Munto<sup>1</sup> 

<sup>1</sup>Universidade Estadual Paulista, Faculdade de Ciências Agrárias e Veterinárias,  
FCAV/Unesp, Jaboticabal, São Paulo, Brasil

<sup>2</sup>Universidade Federal de Jataí (Unidade Acadêmica de Ciências Agrárias - CIAGRA - UFJ),  
Jataí, Goiás, Brasil

### ABSTRACT

The aim of this study was to evaluate the precision of a new surgical drill guide model printed in 3D to assist in directing cervical transpedicular screw placement. Five canine cadavers underwent computed tomography (CT). C5 and C6 cervical vertebrae were exported to three-dimensional (3D) reconstruction software, which allowed the creation of an animal-specific virtual perforation surgical guide (3DSDG) based on the safe corridor of the vertebral pedicle for placement of 2.7 mm screws. The 3DSDG were printed in 3D by the SLA method. Pedicular screws were applied with the aid of the 3DSDG in cadaveric vertebrae (specimens) and ABS-printed biomodels. After implantation, a CT scan was performed on the specimens and biomodels, the images were exported to a program to assess the transverse angle of the perforations. There was no difference between the screw trajectories angles in the species ( $p > 0.05$ ) and biomodels ( $p > 0.05$ ). The evaluation of screw trajectories by the three-dimensional reconstruction method and by computed tomography also showed no significant differences ( $p > 0.05$ ). Our hypothesis was confirmed once the 3D-printed animal-specific drill guide can potentially help guide the drill for screw drilling in the caudal cervical vertebral pedicle in dogs.

Keywords: cervical pedicle, template, canine, cervical spine, patient-specific drilling guide, vertebra

### RESUMO

O objetivo deste estudo foi avaliar a precisão de novo modelo de guia de broca cirúrgica impresso em 3D para auxiliar no direcionamento da colocação do parafuso cervical transpedicular. Cinco cadáveres caninos foram submetidos à tomografia computadorizada (TC). As vértebras cervicais C5 e C6 foram exportadas para um software de reconstrução tridimensional (3D), que permitiu a criação de um guia cirúrgico de perfuração virtual animal-específico (3DSDG) baseado no corredor seguro do pedículo vertebral para colocação de parafusos de 2,7mm. Os 3DSDG foram impressos em 3D pelo método SLA. Parafusos pediculares foram aplicados com auxílio do 3DSDG em vértebras cadavéricas (espécimes) e biomodelos impressos em ABS. Após a implantação, foi realizada uma tomografia computadorizada nos espécimes e nos biomodelos, e as imagens foram exportadas para um programa para avaliar o ângulo transversal das perfurações. Não houve diferença entre os ângulos das trajetórias dos parafusos nas espécies ( $P > 0,05$ ) e nos biomodelos ( $P > 0,05$ ). A avaliação das trajetórias dos parafusos pelo método de reconstrução tridimensional e pela tomografia computadorizada também não apresentou diferenças significativas ( $P > 0,05$ ). A hipótese aqui apresentada foi confirmada, uma vez que o guia de broca específico para animais impresso em 3D pode potencialmente ajudar a guiar a broca para perfuração do parafuso no pedículo vertebral cervical caudal em cães.

Palavras-chave: pedículo cervical, template, canino, coluna cervical, guia de perfuração específico do paciente, vértebra

---

Corresponding author: [laissargi@hotmail.com](mailto:laissargi@hotmail.com)

Submitted: August 21, 2023. Accepted: January 12, 2024.

## INTRODUCTION

Surgical stabilization of the cervical spine in dogs is indicated for the treatment of several conditions, including trauma (fractures and dislocations), congenital malformations (e.g., atlantoaxial instability), degenerative diseases (e.g., cervical spondylomyelopathy), and neoplasms (Wong *et al.*, 2007; Klatzkow *et al.*, 2018; Fernandes *et al.*, 2019, Tuan *et al.*, 2019). Vertebral fixations are achieved by means of pins or screws placed inside the pedicles or vertebral body connected by PMMA and stainless steel or titanium plates (McKee *et al.*, 1999; Trotter, 2009; Adrega *et al.*, 2010).

The use of pedicle screws in the cervical spine in human medicine has increased significantly in the past decade because of its superior biomechanical properties and satisfactory results (Kothe *et al.*, 2004; Johnston *et al.*, 2006). However, their use may present an iatrogenic risk to damage to vital structures, including the vertebral artery, nerve roots, and spinal cord (Chazono *et al.*, 2006; Mathew *et al.*, 2013). In veterinary medicine, anatomical variations in different canine breeds and associated with vertebral malformations render precise implant placement an even greater challenge (Watine *et al.*, 2006). In a cadaveric study comparing the biomechanics of bicortical pins and monocortical screws with PMMA placed freehand in the cervical spine of dogs, 100% of the bicortical pins breached the vertebral canal, and a much lower incidence was observed with monocortical screw fixation (Hettlich *et al.*, 2013).

Fluoroscopic guidance and the use of neuronavigation systems considerably improve implant placement accuracy compared to the freehand technique since they allow the projection of moving images and in real time (Du *et al.*, 2018; Fichtner *et al.*, 2018; Lin *et al.*, 2020). Nonetheless, this method exposes the surgeon and the patient to significant levels of radiation (Singer, 2005). Moreover, the technique has a high financial cost, limiting the application of these technologies in veterinary medicine. Thus, freehand implant placement is common in spinal fixation surgeries, even though it can result in iatrogenic injury (Corlazzoli, 2008; Hamilton-Bennett *et al.*, 2018).

With the more accessible costs of computed tomography (CT) equipment and advancements in biomedical engineering, prototyping technologies have gained space and comprise a promising resource in assisting in the planning and execution of complex spine surgeries, enabling the construction of three-dimensional models from data obtained by CT (Wu *et al.*, 2015; Tack *et al.*, 2016).

Our hypothesis was that a 3D printing technique could be used to build drill guides for the placement of cervical transpedicular screws in predetermined and secure implantation corridors. In addition, the adequate placement of the screw in the vertebral pedicle allows more rigid and stable fixation, in addition to minimizing complications such as cervical instability, screw pull-out, or pedicle fractures (Tang *et al.*, 2014). The aim of the present study was to evaluate the accuracy of the angles obtained after pedicle screw placement in the fifth and sixth cervical vertebrae of canine cadavers and biomodels by means of CT with the aid of a 3D-printed drill guide.

## MATERIAL AND METHODS

Five adult canine cadavers weighing between 35 to 48kg euthanized for reasons unrelated to this study were obtained as approved by the institution's animal care and use committee (no 017144/18). Previous radiographs were performed to rule out congenital anomalies, traumas, bone neoplasms, and discospondylitis. Meticulous disarticulation was carried out between the atlas and axis and between T2-T3, preserving all adjacent cervical muscles, joints, intervertebral discs, and the nuchal ligament from C2 to T2. The vertebral segments were then wrapped in saline-soaked towels and frozen at  $-18^{\circ}\text{C}$ . All specimens were thawed at room temperature 24 hours before use.

A contiguous 1-mm slice CT scan (Shimadzu SCT -7800 CT, Kyoto, Japan) with 1 mm-thick fine cuts was conducted in each specimen. The two-dimensional sequential tomography images obtained in DICOM format were exported to the 3DSlicer software (Surgical Planning Laboratory, Boston, MA, USA) for three-dimensional reconstruction, providing us with a representation of C5 and C6 in a triangulated mesh.

*Precision and trajectory...*

The 3D objects were then exported to another software (Blender, Amsterdam, Netherlands) to create the virtual model of the 3DSDG, enabling the precise planning of the trajectory of each perforation for pedicle screw entry according to the specific vertebral peculiarities of each dog (Fig. 1).

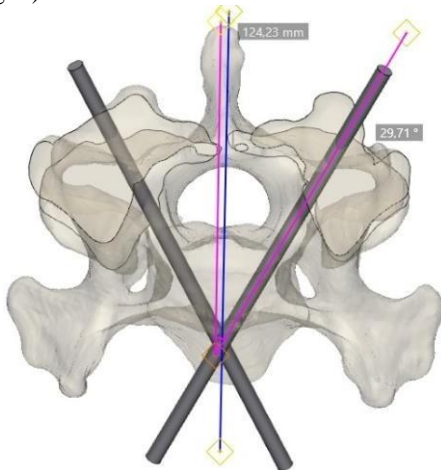


Figure 1. Illustrative computer image of 3D reconstruction of the optimum trajectory determination of the right pedicle screw, with virtual pins, of a canine cadaver's C5 vertebra sectioned in the transverse plane. The blue vertical line corresponds to the midline of the plane that divides the vertebral body, the spinal canal, and the spinous process (sagittal axis). The pink lines refer to the pre-defined pedicular screw orientation angle, based on the vertebral sagittal plane.

Two paths for 2.0-mm drill bits were established for drilling the right and left pedicles of C5 and C6, respectively. The drill guide's contact surface was compatible with the ventral portion of the C5 and C6 vertebral bodies and, therefore, fit perfectly on the bone surface, with two perforation holes, each directed in the orientation of the vertebral pedicles (Fig. 2).

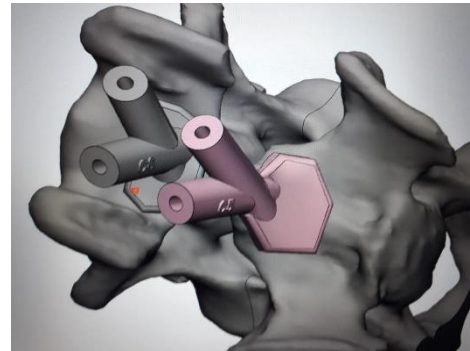


Figure 2. Computer image illustrating the virtual allocation of the 3DSDG on the ventral surface of the C5 and C6 vertebral bodies.

The trajectories of the screws were determined in order to go through the maximum bone stock in the pedicles of C5 and C6 of each specimen. After generating the 3DSDG and virtual drill guidelines, cross-sections were made showing the drill orientations, and the images were saved in a JPEG (Joint Photographic Experts Group) file for later planned angle measurement using the OptiMed software (British Columbia, Canada) (Fig. 3).

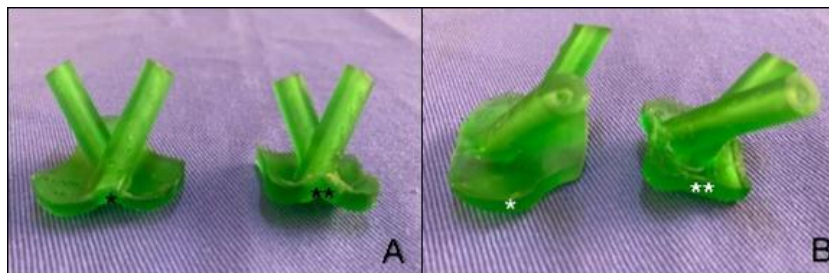


Figure 3. Photographic image of the 3D printed animal-specific drill guide. A, Caudal view of the 3DSDG. B, Lateral view of the 3DSDG. (\*) refers to the corresponding 3DSDG of the C5 vertebra. (\*\*\*) refers to the 3DSDG of the C6 vertebra.

The drill guide models were exported to an STL (Standard Tessellation Language) file and 3D printed with ABS material using a 3D printer (UP 3D Mini 2 ES, Beijing Tiertime Technology Co. Ltd., Pequim, China). A 3D printed biomodels composed of the vertebral bodies of C5 and C6 based on the cadavers was also

produced to simulate the placement of the guides and drilling procedure (Fig. 2). A method known as Direct Light Projection (DLP) was conducted for the printing of the 3DSDG; Fused Deposition Modeling (FDM) was performed for the printing of the biomodels.

Surgery was performed by an experienced surgeon (TASSR) with expertise in spinal surgery and vertebral body screw placement. The specimens were thawed at room temperature, placed in supine position, and covered with surgical field cloths, simulating *in vivo* surgery. An incision was made in the cervical midline to expose the caudal vertebral structures of C5 and C6. The *longus colli* muscles were retracted, and the vertebral bodies and intervertebral discs were completely exposed. The removal of the soft tissues was conducted meticulously to ensure full and firm bone contact with the 3DSDG. The specific 3DSDG positioning location for each C5 and C6 vertebrae was on the ventral surface of the vertebral body of the specimens and biomodels, and guided drilling was carried out using a 2.0 mm-diameter drill bit to create a pilot hole that would accommodate a 2.7-mm cortical screw. The permanence of the first drill bit in the orifice was essential to stabilize the guide to the vertebra, assisting in the precision of the orientation of the second perforation. The drill guidelines were planned so that the drill bits would not touch each other inside the vertebral body, favoring the permanence of both at the same time. After drilling, the drill bits and 3DSDG were removed, exposing the holes for implanting the 2.7 mm-diameter titanium pedicle screws.

Evaluation of the precision of insertion of the pedicle screws in the specimens and biomodels.

The specimens and biomodels with implanted pedicle screws were submitted to a contiguous 1-mm slice CT scan (Shimadzu SCT -7800 CT, Kyoto, Japan). The 3DSlicer software (Surgical Planning Laboratory, Boston, MA, USA) was used for the three-dimensional computational reconstruction of the DICOM files of the specimens' and biomodels' cervical vertebrae. Cross-sections were made, exposing the orientation of the screws. The images were saved in a JPEG file and transferred to the OptiMed program (British Columbia, Canada), which enabled the measurement of the cervical vertebrae for the comparative assessment of the pedicle screws' trajectory in the virtual planning with that of the pedicle screws inserted in the specimens and biomodels. Such comparison allowed us to evaluate the angle in relation to the sagittal plane of the computational perforation and post-implantation guidelines.

The sagittal vertebral axis is a line that divides the vertebral body, the spinal canal, and the spinous process. The screw implantation angle was defined as the angle formed by the axis of the pedicular screw and the sagittal vertebral axis of the respective vertebral body, as described by Mathew *et al.* (2013) two methods were adopted in order to measure the angles: three-dimensional computational reconstruction and computed tomography measurements after implantation (Fig. 4).

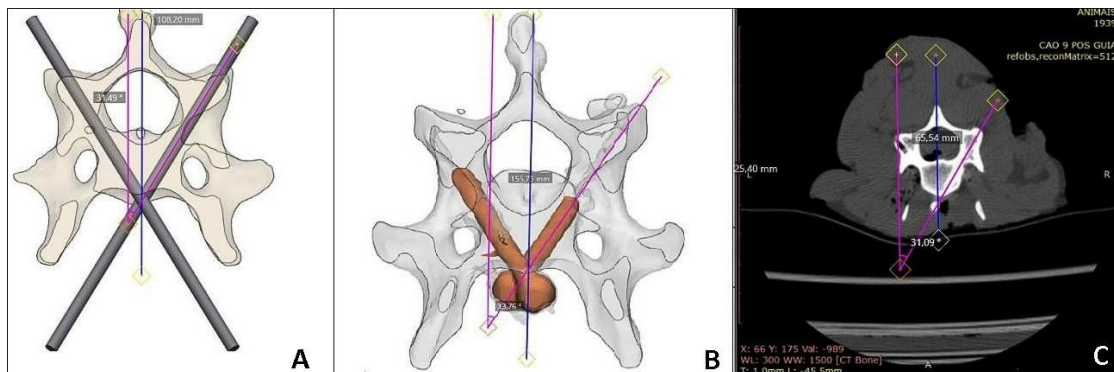


Figure 4. The pedicle screw implantation orientation in the C6 vertebra from canine cadavers. A, Illustrative image of the angulation of the planned computational path of the pedicle screws. B, Illustrative image of the 3D reconstruction of the screw trajectory after application of the 3DSDG. C, Illustrative image of the tomographic image after application of the animal-specific 3DSDG. The blue lines in A, B, and C correspond to the midline that divides the vertebral body, the spinal canal, and the spinous process (sagittal axis). The pink lines in A, B, and C refer to the sagittal angle of the pedicle screw, defined as the axis of the pedicle screw in relation to the sagittal vertebral axis of the respective vertebral body.



Statistical analyses were performed using the R software (version 3.6.3) and the Prism (Prism version 8.4.2; GraphPad Software, La Jolla, California). The angle of the screw's trajectory in each vertebra was assessed by the Kruskal-Wallis test, and the comparisons regarding the angles obtained between the cadaver and the prototype and the evaluation method, by means of reconstruction and tomography, were evaluated using the Friedman test. The resulting values for each variable are shown as median  $\pm$  interquartile range (IQR).

## RESULTS

Altogether, the trajectories of forty pedicle screws measuring 2.7 mm in diameter inserted in the cervical spine specimens of the canine cadavers (n=20) and their respective biomodels (n=20) were evaluated. The 3DSDG proved to be feasible, with easy adjustments on the surface of the vertebral body of both the specimens (Fig 5) and the biomodels (Fig 6).

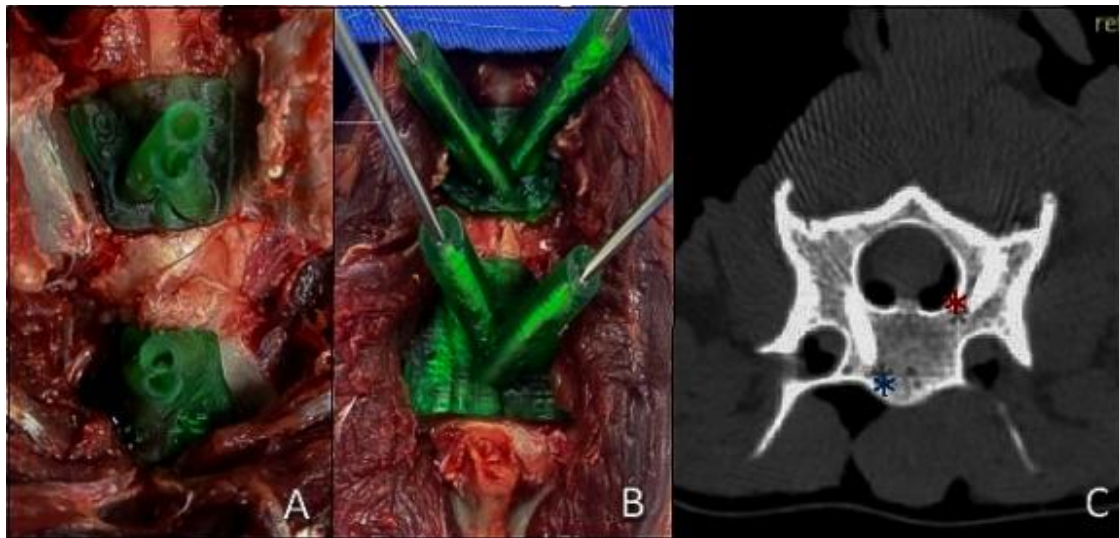


Figure 5. Photographic images of a canine cadaver's cervical spine specimen with the 3DSDG. A, 3DSDG ventrally coupled to the surface of the C5 and C6 vertebral bodies. B, Simulation of drilling guided by the 3DSDG with the aid of 2.0 mm-diameter drills. C, Trajectory of the pedicle screw in the specimen's C5 vertebra, confirmed by computed tomography, demonstrated by the red asterisk (\*) on the right side and the blue asterisk (\*) on the left side.

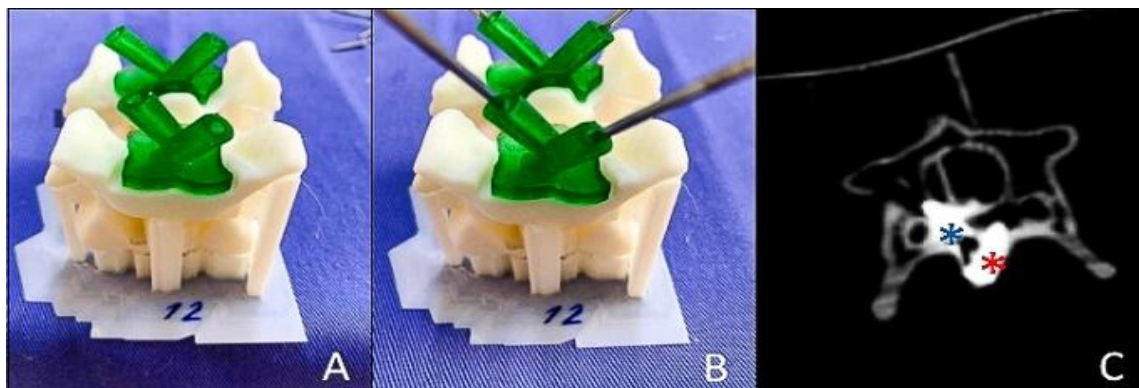


Figure 6. Photographic images of a canine biomodel with the 3D printed animal-specific drill guide. A, 3DSDG ventrally coupled to the surface of the vertebral body of C5 and C6. B, Simulation of drilling guided by the 3DSDG with the aid of 2.0 mm-diameter drills. C, Trajectory of the pedicle screw in the C5 vertebra of the biomodel, confirmed with computed tomography, demonstrated by the red asterisk (\*) on the right side and the blue asterisk (\*) on the left side.

No perforations in the spinal canal were observed by postoperative CT. Also, there were no significant differences in the mean angles of the screw trajectories applied to the C5 vertebra on the right side ( $p=0.479$ ), C5 on the left side ( $p=0.784$ ), C6 on the right side ( $p=0.430$ ), and C6 on the left side ( $p=0.577$ ) in the virtual angle

and between the trajectories of the specimens and biomodels. There was no effect regarding the evaluation on the cadaver or the prototype, nor by using the three-dimensional reconstruction method or computed tomography ( $p>0.05$ ) (Table 1).

Table 1. Median  $\pm$  interquartile range of the angles ( $^{\circ}$ ) of the pedicle screw trajectories in the C5 and C6 vertebrae of the virtual, cadavers and biomodel evaluated by three-dimensional reconstruction and tomographic imaging

	Virtual	Reconstruction		Tomography		P-value		
		Cadavers	Biomodels	Cadavers	Biomodels	V $\times$ C $\times$ B*	C $\times$ B**	Re $\times$ T***
<b>C5</b>								
R	30.53 $\pm$ 7.21	33.80 $\pm$ 6.89	28.00 $\pm$ 3.61	31.18 $\pm$ 6.33	30.27 $\pm$ 5.58	0.479	0.217	0.739
L	33.61 $\pm$ 5.20	26.73 $\pm$ 4.07	32.56 $\pm$ 12.15	24.25 $\pm$ 13.48	31.15 $\pm$ 19.02	0.784	0.684	0.684
<b>C6</b>								
R	31.49 $\pm$ 6.08	26.06 $\pm$ 9.75	25.86 $\pm$ 2.60	24.66 $\pm$ 9.71	32.49 $\pm$ 3.79	0.430	0.435	0.853
L	31.82 $\pm$ 3.05	33.89 $\pm$ 7.98	25.65 $\pm$ 6.02	34.27 $\pm$ 5.02	30.78 $\pm$ 6.81	0.577	0.384	0.161

C5: fifth cervical vertebra, C6: sixth cervical vertebra, R: right, L: left, V: virtual, C: cadavers, Re: reconstruction; T, tomography.

\* = effects of the virtual, cadavers and biomodels, evaluated using the Kruskal-Wallis test.

\*\* = effects of the type of assessment (cadavers vs biomodels), evaluated using the Friedman test.

\*\*\* = effects of the type of assessment (Reconstruction vs Tomography), evaluated using the Friedman test.

$P<0.05$

The overall mean angle of screw deviation in the C5 and C6 vertebrae ranged from 0.36 to 4.29 degrees in the ex vivo and 3.53 to 5.20 degrees in the biomodel using the 3D reconstruction evaluation method (Table 2). Based on the CT

evaluation method, the overall mean angle of screw deviation varied between 2.8 and 4.99 degrees in the specimens and 1.68 to 7.7 degrees in the biomodels.

Table 2. Mean $\pm$ SD of the sagittal angles ( $^{\circ}$ ) of the pedicle screw trajectories in relation to the virtual angle

	3D computational reconstruction		Computed Tomography	
	Cadavers	Biomodels	Cadavers	Biomodels
<b>C5</b>				
Right	-0.36 $\pm$ 6.28	5.20 $\pm$ 4.05	3.22 $\pm$ 3.40	2.95 $\pm$ 5.02
Left	3.25 $\pm$ 5.18	4.76 $\pm$ 4.73	4.99 $\pm$ 6.94	7.75 $\pm$ 11.4
<b>C6</b>				
Right	1.86 $\pm$ 8.84	3.53 $\pm$ 3.86	4.91 $\pm$ 6.93	-1.37 $\pm$ .76
Left	0.58 $\pm$ 2.47	4.29 $\pm$ 3.99	-2.82 $\pm$ 3.18	1.68 $\pm$ 8.39

## DISCUSSION

The obtained results evidence the feasibility of using a three-dimensionally printed animal-

specific drill guide to direct the trajectory of pedicle screws in the caudal cervical region of dogs. This study enabled the precise and safe perforation of 40 pedicle screws in 5 dog

cadavers and their respective biomodels. The drilling results obtained with the aid of the 3DSDG would be considered acceptable if they were created in the clinical setting.

Mariani *et al.* (2021) evaluated 3D printed drill guides for perforating the T8 to T13 vertebrae of 5 canine cadavers. The authors found a mean angular deviation of 5.1° (range, 1.5°-10.8°), and no unwanted breaching was observed in the subjects' bones. In the present study, although it was aimed at cervical vertebrae, similar results were found regarding mean angular deviation (Tab 2). Hamilton-Bennett *et al.* (2018) investigated the drilling of 32 screws in the cervical spine and reported that most (29/32) of the screws were allocated without evidence of spinal canal rupture and only to an extent of less than 2 mm (9.4%). Fujioka *et al.* (2019) analyzed the perforation of 29 screws in canine thoracolumbar vertebrae and also verified that 89.6% of the screws were inserted without evidence of breaching the spinal canal. The general mean deviation of the screws was 1.16 ± 0.56 mm.

The deviations in screw angles may be related to intrinsic factors regarding the 3DSDG application process. According to Fujioka *et al.* (2019), the bur load during the procedure can generate micromovements during drilling sufficient to provide a minimum deviation. In addition, the drill bit must be extremely sharp since the resistance of the drill's oscillation upon insertion is sufficient to deflect perforation. Mariani *et al.* (2021) used a 2.5-mm bur without drilling a pilot hole for screws in the thoracolumbar spine of dogs with the aid of a surgical guide and reported that even if the bur were restricted by the guide, there is a possibility of drill slip. In the present study, to prevent the displacement of the 3DSDG, temporal fixation was performed in one of the guide's holes with the aid of a pin to initiate drilling on the contralateral side.

The purpose of using biomodels in this study was to promote a counterproof to the guide's application, given that bone biomodels are reliable copies of the anatomical structure obtained from imaging tests (Lohfeld *et al.*, 2005). In the present study, the deviations in the screw trajectories between the biomodels and the specimens did not show any significant

differences. Bone models, however, do not have adjacent soft tissue, rendering this study model limited since, in practice, it is essential that all soft tissues adjacent to and on the vertebral surface be removed. The adequate dissection of soft tissue allows us to optimize the adjustment of the guide in the vertebral body, thus avoiding the incorrect targeting of pilot holes in the cadavers (Hamilton-Bennett *et al.*, 2018). The presence of adjacent soft tissue herein did not hinder the application of the 3DSDG since it was a cadaveric study, a fact that enabled greater dissection without complications. In clinical studies, on the other hand, it can be stated that the removal of soft tissue is one of the main challenges when 3DSDG s are applied (Azimifar *et al.*, 2019).

Computed tomography-related components should be considered for the evaluation of screw trajectories. Minimization of artifacts by using a titanium screw instead of stainless steel are details that have improved accuracy when determining the position of the pedicle screw (Hamilton-Bennett *et al.*, 2018; Fujioka *et al.*, 2019). Also, the cut thicknesses of tomographic images influence the loss of image definition (Fujioka *et al.*, 2019). In this context, we opted for 1.0-mm cuts since larger thicknesses would result in the loss of image definition. In addition, the inclination of the table frame should be considered because it influences the accurate measurement of the screw (Kim *et al.*, 2003). Mariani *et al.* (2021) reported, in their study, that the pre- and postoperative computed tomography images were not captured at identical cutting sites, a fact that can lead to a small amount of error in angle measurement.

To date, some studies have described different conformations of guides with high accuracy verified by postoperative CT evaluation. However, there is no consensus on the design of a safer and more accurate guide model in humans (Pijpker *et al.*, 2019), the same applies to veterinary medicine. The 3DSDG model, in this study, was designed to cover the entire ventral surface of the vertebral body so that it could be attached to the bone with bilateral perforations. The placement of the guide only for fitting, with vertebral pedicle orientation, without vertebral covering, can contribute to imprecision in the procedure (Kamishina *et al.*, 2019).

Most studies are limited to measuring the screw trajectory based on CT (Hamilton-Bennett *et al.*, 2018; Fujioka *et al.*, 2019; Kamishina *et al.*, 2019; Fujioka *et al.*, 2020). In the present study, in addition to the measurements conducted using tomographic images, we also measured images using 3D reconstruction based on the images acquired by CT. Although there was no statistically significant difference, discrepancies in the mean values were observed. In this context, it can be suggested that specific studies on the accuracy of measuring 3D reconstruction with tomographic imaging are necessary.

The insertion of screws in the vertebral pedicle of the cervical spine in dogs is challenging due to the narrow implant corridor, and serious consequences can occur due to failure in screw fixation, such as damage to vascularization or penetration into the spinal canal (Corlazzoli, 2008). The present study demonstrates the importance of planning the specific angulation for the patient according to their anatomical particularities in order to avoid possible complications. In the study by Corlazzoli (2008), a considerable variation was identified among dogs of the same breed and their vertebrae. This can be explained by anatomical differences between each third of each vertebra and among dogs of the same breed.

The main limitation of our study was that a clinical trial was not performed, thus hindering the observation of possible transoperative complications related primarily to damage to blood vessels and short- and long-term postoperative complications.

### CONCLUSION

The model of the surgical drill guide specific for the animal developed in the present study was favorable in directing the drill to insert the screw in the caudal cervical vertebral pedicle. The use of 3DSDG should facilitate the surgical procedure of cervical stabilization in dogs, although it should not be an alternative for inexperienced surgeons.

### ACKNOWLEDGEMENTS

This study was supported by the São Paulo Research Foundation (FAPESP, no 2018/248594).

### REFERENCES

- ADREGA, C.S.; BERNARD, F.; BARDET, J.F. Caudal cervical arthrodesis using a distractable fusion cage in a dog. *Vet. Comp. Orthop. Traumatol.*, v.23, p.209-213, 2010.
- AZIMIFAR, F.; HASSANI, K.; HOSSEIN SAVEH, A.; IZADI, F. A new template and teleoperation system for human-guided spine surgery. *Artif. Organs*, v.43, p.424-434, 2019.
- CHAZONO, M.; SOSHI, S.; INOUE, T.; KIDA, Y.; USHIKU, C. Anatomical considerations for cervical pedicle screw insertion: the use of multiplanar computerized tomography reconstruction measurements. *J. Neurosurg. Spine*, v.4, p.472-477, 2006.
- CORLAZZOLI, D. Bicortical implant insertion in caudal cervical spondylomyelopathy: a computed tomography simulation in affected Doberman Pinschers. *Vet. Surg.*, v.37, p.178-185, 2008.
- DU, J.P.; FAN, Y.; WU, Q.N.; ZHANG, J. *et al.* Accuracy of pedicle screw insertion among 3 image-guided navigation systems: systematic review and meta-analysis. *World Neurosurg.*, v.109, p.24-30, 2018.
- FERNANDES, R.; FITZPATRICK, N.; RUSBRIDGE, C.; ROSE, J. *et al.* Cervical vertebral malformations in 9 dogs: radiological findings, treatment options and outcomes. *Ir. Vet. J.*, v.72, p.1-13, 2019.
- FICHTNER, J.; HOFMANN, N.; RIENMÜLLER, A.; BUCHMANN, N. *et al.* Revision rate of misplaced pedicle screws of the thoracolumbar spine—comparison of three-dimensional fluoroscopy navigation with freehand placement: a systematic analysis and review of the literature. *World Neurosurg.*, v.109, p.e24-e32, 2018.
- FUJIOKA, T.; NAKATA, K.; NISHIDA, H.; SUGAWARA, T. *et al.* A novel patient-specific drill guide template for stabilization of thoracolumbar vertebrae of dogs: cadaveric study and clinical cases. *Vet. Surg.*, v.48, p.336-342, 2019.
- FUJIOKA, T.; NAKATA, K.; NAKANO, Y.; NOZUE, Y. *et al.* Efficacy of a patient-specific drill guide template system for lumbosacral junction fixation in medium and small dogs: cadaveric study and clinical cases. *Front. Vet. Sci.*, v.6, p.494, 2020.
- HAMILTON-BENNETT, S.E.; OXLEY, B.; BEHR, S. Accuracy of a patient-specific 3D printed drill guide for placement of cervical transpedicular screws. *Vet. Surg.*, v.47, p.236-242, 2018.



*Precision and trajectory...*

- HETTLICH, B.F.; ALLEN, M.J.; PASCETTA, D.; FOSGATE, G.T. *et al.* Biomechanical comparison between bicortical pin and monocortical screw/polymethylmethacrylate constructs in the cadaveric canine cervical vertebral column. *Vet. Surg.*, v.42, p.693-700, 2013.
- JOHNSTON, T.L.; KARAIKOVIC, E.E.; LAUTENSCHLAGER, E.P.; MARCU, D. Cervical pedicle screws vs. lateral mass screws: uniplanar fatigue analysis and residual pullout strengths. *Spine J.*, v.6, p.667-672, 2006.
- KAMISHINA, H.; SUGAWARA, T.; NAKATA, K.; NISHIDA, H. *et al.* Clinical application of 3D printing technology to the surgical treatment of atlantoaxial subluxation in small breed dogs. *PLoS One*, v.14, p.e0216445, 2019.
- KIM, H.S.; HELLER, J.G.; HUDGINS, P.A.; FOUNTAIN, J.A. The accuracy of computed tomography in assessing cervical pedicle screw placement. *Spine*, v.28, p.2441-2446, 2003.
- KLATZKOW, S.; JOHNSON, M.D.; JAMES, M.; CARRERA-JUSTIZ, S. Ventral stabilization of a T2-T3 vertebral luxation via median sternotomy in a dog. *Case Rep. Vet. Med.*, v.2018, p.152394, 2018.
- KOTHE, R.; RUTHER, W.; SCHNEIDER, E.; LINKE, B. Biomechanical analysis of transpedicular screw fixation in the subaxial cervical spine. *Spine*, v.29, p.1869-1875, 2004.
- LIN, C.W.; CHANG, C.C.; CHEN, H.T.; CHEN, Y.J. *et al.* 3D real-time image-guided navigation spine corpectomy with Ultrasonic bone cutter. *World Neurosurg.*, v.135, p.197-204, 2020.
- LOHFELD, S.; BARRON, V.; MCHUGH, PE. Biomodels of bone: a review. *Ann. Biomed. Eng.*, v.33, p.1295-1311, 2005.
- MARIANI, C.L.; ZLOTNICK, J.A.; HARRYSSON, O.; MARCELLIN-LITTLE, D.J. *et al.* Accuracy of three-dimensionally printed animal-specific drill guides for implant placement in canine thoracic vertebrae: a cadaveric study. *Vet. Surg.*, v.50, p.294-302, 2021.
- MATHEW, J.E.; MOK, K.; GOULET, B. Pedicle violation and navigational errors in pedicle screw insertion using the intraoperative O-arm: a preliminary report. *Int. J. Spine Surg.*, v.7, p.e88-e94, 2013.
- MCKEE, W.M.; BUTTERWORTH, S.J.; SCOTT, H.W. Management of cervical spondylopathy-associated intervertebral disc protrusions using metal washers in 78 dogs. *J. Small Anim. Pract.*, v.40, p.465-472, 1999.
- PIJPKER, P.A.J.; KRAEIMA, J.; WITJES, M.J.H. *et al.* Accuracy assessment of pedicle and lateral mass screw insertion assisted by customized 3D-Printed drill guides: a human cadaver study. *Oper Neurosurg. (Hagerstown)*, v.16, p.94-102, 2019.
- SINGER, G. Occupational radiation exposure to the surgeon. *J. Am. Acad. Orthop. Surg.*, v.13, p.69-76, 2005.
- TACK, P.; VICTOR, J.; GEMMEL, P.; ANNEMANS, L. 3D-printing techniques in a medical setting: a systematic literature review. *Biomed. Eng. Online*, v.15, p.1-21, 2016.
- TANG, J.; ZHU, Z.; SUI, T.; KONG, D. *et al.* Position and complications of pedicle screw insertion with or without image-navigation techniques in the thoracolumbar spine: A meta-analysis of comparative studies. *J. Biomed. Res.*, v.28, p.228, 2014.
- TROTTER, E.J. Cervical spine locking plate fixation for treatment of cervical spondylotic myelopathy in large breed dogs. *Vet. Surg.*, v.38, p.705-718, 2009.
- TUAN, J.; SOLANO, M.A.; FITZPATRICK, N. Ventral distraction-stabilization in 5 continuous sites for the treatment of cervical spondylomyelopathy in a Great Dane. *Vet. Surg.*, v.48, p.607-614, 2019.
- WATINE, S.; CABASSU, J.P.; CATHELAND, S.; BROCHIER, L. *et al.* Computed tomography study of implantation corridors in canine vertebrae. *J. Small Anim. Pract.*, v.47, p.651-657, 2006.
- WONG, M.A.; MARIANI, C.L.; POWE, J.R.; CLEMMONS, R.M. Teratoma in the cervical spinal cord of a dog. *J. Am. Anim. Hosp. Assoc.*, v.43, p.292-297, 2007.
- WU, A.M.; SHAO, Z.X.; WANG, J.S.; YANG, X.D. *et al.* The accuracy of a method for printing three-dimensional spinal models. *PLoS One*, v.10, p.e0124291, 2015.